Coherent re-emission of gamma -quanta in the forward direction after a stepwise change of the energy of nuclear excitation

1993 J. Phys.: Condens. Matter 5 1557

(http://iopscience.iop.org/0953-8984/5/10/013)

J. Phys.: Condens. Matter 5 (1993) 1557–1580. Printed in the UK

Coherent re-emission of γ-quanta in the forward direction after a stepwise change of the energy of nuclear excitation

Yu V Shvyd'ko, S L Popov and G V Smirnov
RSC 'Kurchatov Institute', Moscow, 123182, Russia

Received 4 August 1992, in final form 15 October 1992

Abstract. The re-emission of γ-quanta in the forward direction by an ensemble of excited nuclei after abruptly changing the energy of the nuclear excitation is studied. A sublevel of the 14.4 keV excited state with a definite spin projection of ^{57}Fe nuclei in a magnetic $^{57}FeBO_3$ crystal is selectively populated. The abrupt change of the energy of the excited nuclear state is achieved by fast ($\leqslant$ 5 ns) reversal of the hyperfine (HF) magnetic field direction at the nuclei. The nuclear target was a black absorber prior to HF field reversal. A short (about 10 ns) intense flash followed by beats of γ-radiation intensity is detected with some delay after reversal. The delay of the flash and the beat period depend on the HF nuclear transition excited. The duration of the flash depends on the effective thickness of the nuclear target.

The theory developed interprets the time evolution of the re-emission as a result of the interference of two main spectral components of γ-radiation. The first one has the original frequency, which represents the primary radiation. The second one has a shifted frequency, which represents radiation coherently re-emitted in the forward direction from the nuclear sublevel with energy changed by the HF field reversal. The observations reveal the feasibility of inelastic coherent γ-resonance scattering and demonstrate the enhancement of the radiative channel in the coherent re-emission of γ-radiation in the forward direction.

1. Introduction

The coherent resonance scattering of γ-rays in a system of identical nuclei proceeds via the formation of an intermediate excited state, which spreads over the entire nuclear system [1,2]. In this state there exists a certain probability amplitude for each nucleus to be excited. A space and time correlation of excitation amplitudes among all excited nuclei takes place. The correlation of nuclear excitation amplitudes modifies drastically the properties of γ-resonance scattering (see e.g. reviews [3] and [4] and references therein).

First, it gives rise to directional re-emission of γ-quanta at the decay of the collective nuclear excited state. In a crystal, the nuclei emit γ-quanta coherently in the forward direction and at the Bragg angle. In spatially disordered nuclear systems only coherent re-emission in the forward direction is possible [5,6]. Secondly, the coherence gives rise to a drastic redistribution of the yield of the nuclear reaction products in favour of the radiative channel. The radiative channel dominates in a coherent scattering process while the incoherent channels, like internal conversion, are suppressed [7]. These two features make coherent γ-resonance scattering very important for applications.

0953-8984/93/101557+24$07.50

Resonant γ-quanta scattering by an ensemble of identical nuclei is known to be spatially coherent if the energies of incident and re-emitted γ-quanta are the same, i.e. when elastic scattering takes place [8]. However, it remains an open question whether or not inelastic scattering could be coherent. There are different answers to this question. For instance, nuclear resonant scattering that is accompanied by spin flip is known to be incoherent, because in this process the excitation is localized at a definite nucleus [8,9]. On the other hand, it has been observed that in an ensemble of vibrating nuclei coherent inelastic nuclear scattering is possible [10,11] (hereafter it will also be referred to as coherent nuclear Raman scattering). The obligatory condition for this type of scattering to take place is synchronous vibration of the nuclei [11].

In the present paper we report on the results of an experimental and theoretical study of coherent nuclear Raman scattering under conditions of abrupt change of the energy of the re-emitted radiation by abruptly changing the energy of the intermediate excited nuclear state. Preliminary results and interpretation were published earlier in [12]. The energy of the intermediate state is changed by fast reversal of the hyperfine (HF) magnetic field direction. Spin-flip scattering [9] results in a change of the energy of the re-emitted γ-quanta as well. However, the essential difference is that in spin-flip scattering the energy of the nuclear transition and therefore the energy of the re-emitted γ-quanta change due to accidental spin flip of one of the nuclei. In the case under consideration the nuclear transition energy changes synchronously on each nucleus in the scattering ensemble. This is a necessary condition for coherent nuclear Raman scattering.

In this paper we study coherent scattering in the forward direction. The change of the nuclear transition energy and, consequently, of the re-emitted quanta energy provides an opportunity to distinguish the re-emitted radiation from the primary beam and, thus, to study the properties of inelastic coherent forward scattering by nuclei.

The greater part of the paper is devoted to elaboration of the theory describing the coherent inelastic scattering of resonant radiation in the forward direction by nuclei upon the abrupt reversal of the magnetic HF field direction. The wave equation describing γ-radiation propagation under these conditions is derived. A number of solutions related to the experiment are obtained. The experimental results are compared with calculated theoretical dependences. The theory developed fits the experiment in question adequately.

2. Experiment

2.1. Experimental method and instrumentation

The layout of the experimental set-up is shown in figure 1. The resonant 14.4 keV γ-quanta are scattered by ^{57}Fe nuclei in a $^{57}FeBO_3$ crystal platelet (the target). The crystalline platelet of about 4.5 mm in diameter and of thickness $L_T = 17$ μm was grown from material enriched up to 95% in ^{57}Fe [13]. The spins of the iron atoms are ordered antiferromagnetically in the easy magnetization plane of iron borate. This plane is parallel to the platelet surface. The spins are slightly canted, thus producing a weak ferromagnetic moment perpendicular to the spin directions [14,15]. This moment makes it possible to control the atomic spin orientation in the platelet plane. By applying a weak external magnetic field $H_{c2} = 6$ Oe ($H_{c2} \perp z$), the atomic spins can be aligned with the z axis. The magnetic moment of an iron atom produces the

magnetic field H_{hf} at a nucleus. Figure 1 shows only one of two possible opposite directions of the HF field produced by the magnetic sublattices at the nuclei. The ground and first excited states of the ^{57}Fe nuclei are split due to the hyperfine interaction $-\mu \cdot H_{hf}$ between the nuclear magnetic moment μ and the magnetic field H_{hf} (figure 2(*a*)). M and m in figure 2 denote the quantum numbers of the nuclear magnetic moment projections on the z axis, which is collinear with H_{hf}. Figure 3(*a*) shows the Mössbauer absorption spectrum for the crystal under study.

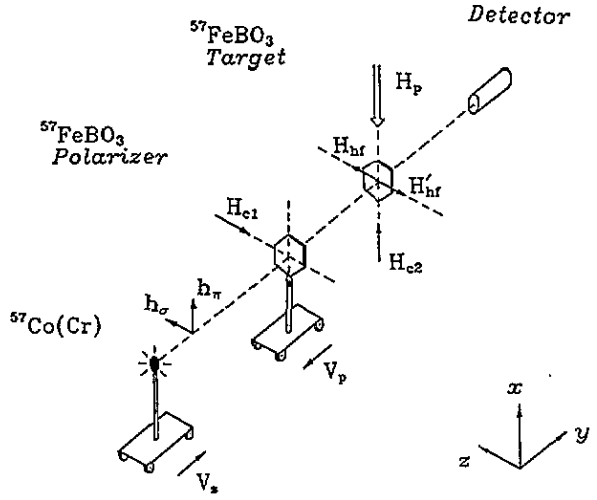

Figure 1. The scheme of the experimental set-up. The hyperfine fields on ^{57}Fe nuclei in the $^{57}FeBO_3$ crystal are inverted ($H_{hf} \rightarrow H'_{hf}$) by abrupt application of the external field H_p. The other designations are given in the text.

The method of changing the nuclear state energy uses the dependence of the hyperfine interaction on the mutual orientation of the HF field and the nuclear spin. For example, by changing instantaneously the HF field direction from H_{hf} to $H'_{hf} = -H_{hf}$, the energy of the HF interaction is changed from $-\mu \cdot H_{hf}$ to $+\mu \cdot H_{hf}$. Note that the abrupt change of the HF field direction does not cause a change of the nuclear magnetic moment μ projection on the z axis. (The relaxation of the nuclear magnetic moment in $FeBO_3$ due to solid-state interactions takes a very long time ($\geqslant 10^{-4}$ s [16]) compared with the characteristic nuclear times τ_0 and τ_L.)

In the experiment the HF field direction is changed by the magnetization reversal of a $^{57}FeBO_3$ crystal. This reversal is caused by the sudden application at time $t = 0$ of the external magnetic field H_p antiparallel to H_{c2}. Note that $H_p = 20$ Oe $\gg H_{c2}$. The reversal occurs over the time $\tau_r \leqslant 5$ ns, which is much shorter than the nuclear lifetime in the excited state ($\tau_0 = 141.1$ ns), and also much shorter than the period of the Larmor spin precession ($\tau_L \simeq 40$ ns) of the ^{57}Fe nuclear spin in the excited state about the HF field in $FeBO_3$. The magnetization reversal time is short owing to the magnetic properties and perfection of the $^{57}FeBO_3$ crystal [17, 18]. The reversed state of magnetization is maintained for 400 ns. During this time the transients of the γ-ray resonant scattering die away. The magnetization reversal is repeated every $T_p = 2$ μs. For a description of the instrumentation used for producing pulsed magnetic fields,

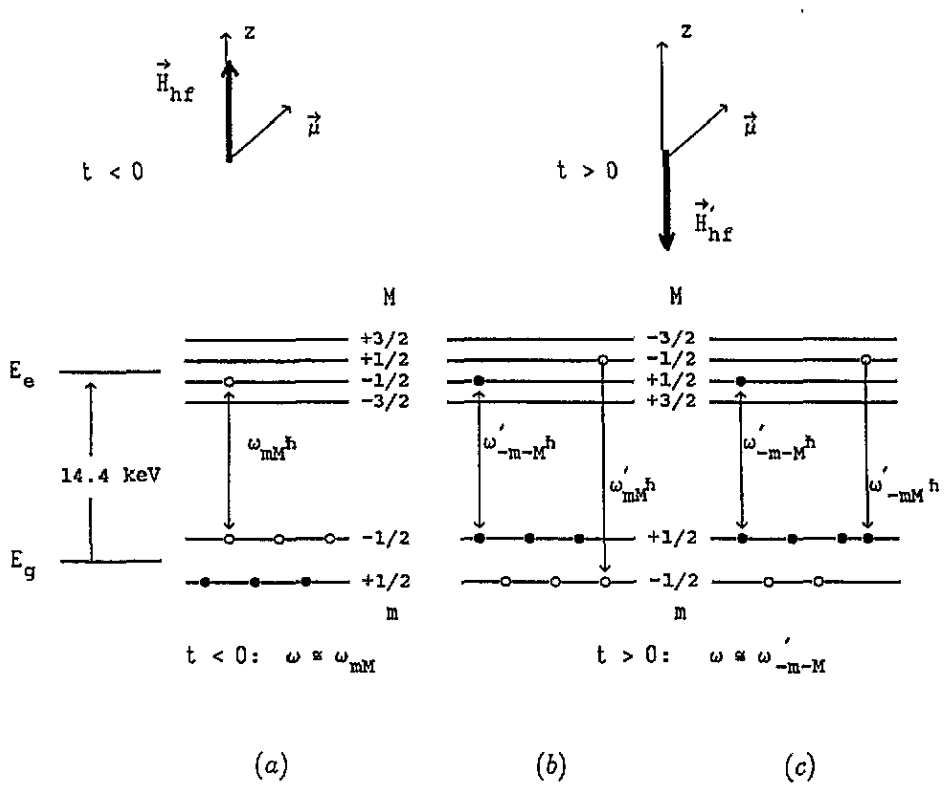

Figure 2. The scheme of the energy levels in the ground and 14.4 keV excited states of ^{57}Fe. (*a*) The incident radiation excites the $m \rightarrow M$ transition and the subsystem of 'white' nuclei prior to HF field reversal ($\boldsymbol{H}_{hf} \rightarrow \boldsymbol{H}'_{hf}$). (*b*), (*c*) The incident radiation excites the $-m \rightarrow -M$ transition and the subsystem of 'black' nuclei after HF field reversal ($\boldsymbol{H}_{hf} \rightarrow \boldsymbol{H}'_{hf}$). Two alternative possibilities for the spontaneous nuclear decay are indicated: (*b*) is coherent and (*c*) is incoherent.

see [18] and references therein. Such frequent magnetization reversal causes heating of the crystal (by 15 K approximately). This heating, in turn, causes a change $\delta\omega_{mM}$ [15] of the nuclear transition frequency compared with the room-temperature value, approximately by ± 0.4 mm s^{-1} for transitions b and e† (see figure 3(*b*)). In addition, the magnetization reversal process excites magnetoacoustic oscillations in the crystal with frequency $\sim 1/T_p = 0.5$ MHz, which cause the resonance lines to broaden, and thus reduces the probability of excitation of the nuclear transitions [19].

The 14.4 keV Mössbauer radiation from the ^{57}Co(Cr) radioactive source propagates along the y axis. The source linewidth is $\Gamma_s = 0.19$ mm s^{-1}. The radiation strikes the crystal perpendicular to the surface. The source is moved at constant velocity V_s, so that the radiation selectively excites one of the $m \rightarrow M$ transitions between the ground state and the first excited state of the ^{57}Fe nuclei in the target (figure 2(*a*)) at frequency ω_{mM}.

† In some cases the $m \rightarrow M$ transitions will be denoted by one letter for simplicity. The correspondence of the two types of designation is presented in figure 3.

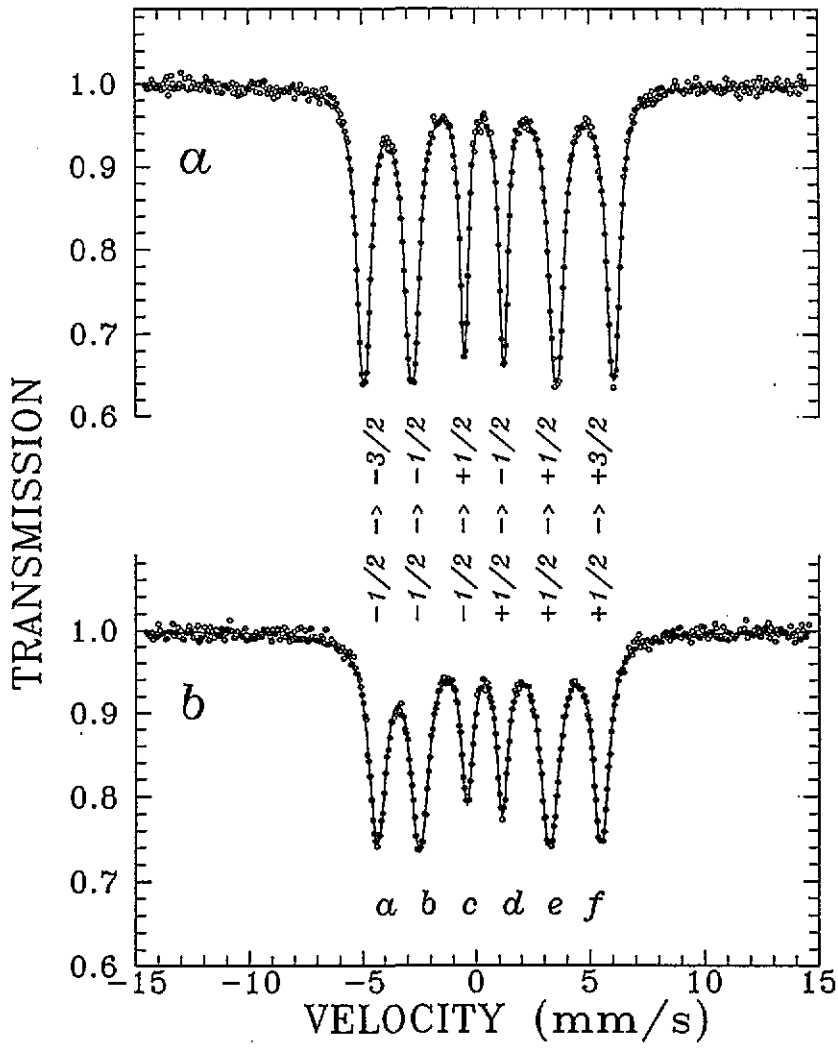

Figure 3. Mössbauer absorption spectra for the $^{57}FeBO_3$ crystal: (*a*) without external perturbations; (*b*) with applied pulsed magnetic field. The broadening of the resonance lines is due to magnetoacoustic vibrations. The shifts of the lines are due to heating in the process of the magnetization reversal.

The nuclei in the crystal, which is magnetized by the constant external field H_{c2}, can interact with one polarization component of γ-radiation only, e.g. the transitions b and e with the h^{σ} component (estimated resonance-absorption factor $m_{b,e}L_T \simeq 44$). The other component traverses the target without interaction with nuclei, thus producing additional background. To reduce the background radiation, a resonant polarizer was installed ahead of the target. For this purpose another $^{57}FeBO_3$ crystal was used. To extract radiation with the required polarization, the polarizer was magnetized by an external magnetic field $H_{c1} = 30$ Oe, which was directed perpendicular to H_{c2}, i.e. $H_{c1} \| z$. The polarizer was at room temperature

(in contrast to the heated target). To be in resonance with the incident radiation the polarizer was moved by another transducer at constant velocity $V_p = -\delta\omega_{mM}$. The polarizer crystal has a thickness $L_p = 30\ \mu$m, which corresponds to a very large resonance-absorption factor, $m_{b,e}L_p \simeq 78$. For this reason it extracted effectively the h^σ component of radiation. The system of two thick $^{57}FeBO_3$ crystals magnetized orthogonally was opaque for incident radiation under steady-state conditions.

The main questions that have been studied experimentally are as follows: (i) Does the spontaneous emission of γ-quanta at shifted frequencies ω'_{mM} and ω'_{-mM} (figures 2(*b*) and (*c*))† proceed coherently in the forward direction? (ii) What are the properties of the inelastic coherent nuclear forward scattering?

To answer these questions the time evolution of γ-radiation emerging from the target after magnetization reversal was measured. The γ-emission was recorded by a method similar to that described in [18,20]. The time resolution of the detector was 5.1 ns. Only γ-radiation emerging within a very small solid angle in the forward direction ($\simeq 5 \times 10^{-4}$ sterad) was detected in the experiment.

2.2. *Experimental results: time evolution of γ-ray re-emission*

Figure 4 shows the time evolution of the intensity of γ-rays emerging from the target in the forward direction. The time $t = 0$ corresponds to the beginning of the magnetization reversal. Each time dependence was measured at a selective excitation of one of the HF transitions in the $^{57}FeBO_3$ crystal. In all three cases an intense short burst of γ-ray emission was observed behind the target after its magnetization reversal. The trivial reason for this burst of radiation is the temporary transparency of the target, which occurs at magnetization reversal. Another reason that is found is a highly directional and enhanced re-emission of γ-quanta by nuclei in the excited state with changed energy. The bursts observed reach and even exceed the incident radiation intensity, indicated by a broken horizontal line. In two cases (figures 3(*a*) and (*b*)) intensity beats are clearly seen. The incident radiation intensity was determined by additional measurements under conditions where the incident radiation frequency was set far off the resonance by moving the source at large velocity $V_s \simeq 10$ mm s^{-1}. The Mössbauer drive of the polarizer was moved at a velocity that tuned the polarizer again to the appropriate resonance $m \rightarrow M$ with the incident radiation.

The observed time evolution curves have nearly the same overall shape for each of the excited transitions, but they do differ in details: (i) The peak intensity of the first burst is reached at different times t_{mM} for excitation of different transitions, earliest in case a and latest in case c: $t_b - t_a = 3.5 \pm 1.2$ ns and $t_c - t_a = 17.5 \pm 1.2$ ns. (ii) The bursts differ in duration $\Delta\tau_{mM}$, being shortest in case b, $\Delta\tau_b = 10.8 \pm 0.5$ ns (FWHM), and longest in case c, $\Delta\tau_c = 21.6 \pm 0.5$ ns. (iii) The beat period T_{mM} in case a, $T_a \simeq 8.2$ ns, is smaller than that in case b, $T_b = 15.5$ ns. The different arrival times t_{mM} (i) and different periods T_{mM} of intensity beats (iii) may result from the interference of two coherent components of γ-radiation with different frequencies. The difference can be determined from the period T_{mM} of the intensity beats. For example, the value $T_b = 15.5$ ns corresponds with good accuracy to the difference in frequencies of the two nuclear transitions $+1/2 \rightarrow +1/2$ and $-1/2 \rightarrow -1/2$, via the relation $T_{mM} = 2\pi/|\omega_{mM} - \omega_{-m-M}|$. Since $\omega_{-m-M} = \omega'_{mM}$ (figures

† Hereafter the prime, e.g. in ω'_{mM}, denotes the changed transition frequency value after the field reversal.

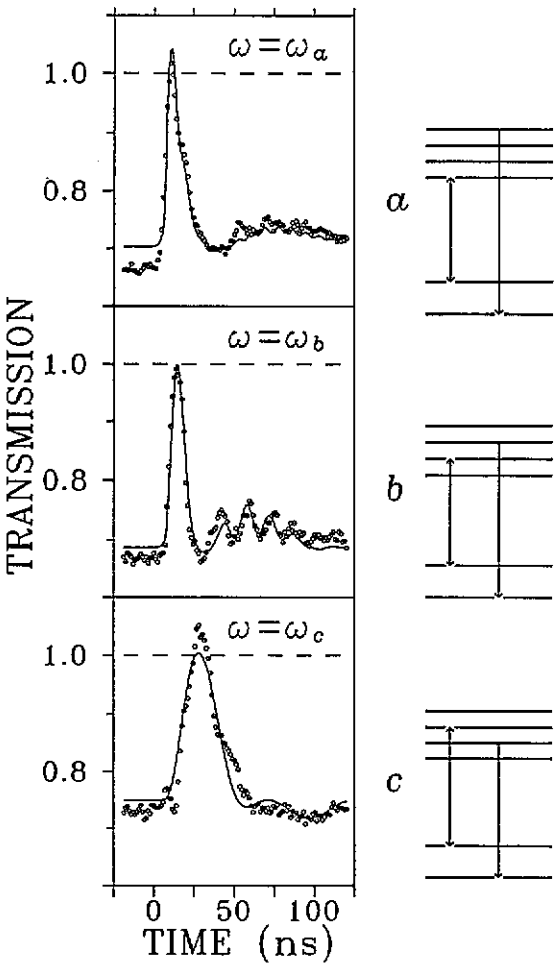

Figure 4. Time evolution of the intensity of γ-rays emerging from the target in the forward direction after excitation of different HF nuclear transitions.

2(*a*) and (*b*)), we can see that the observed time evolutions of radiation emerging from the target after the HF field reversal are shaped by the interference of two radiation components. One component has an incident radiation frequency close to ω_{mM}. The other one has the frequency ω'_{mM}. This component originates from a spontaneous decay of nuclei in the excited state with changed energy (figure 2(*b*)). It is important to note that nuclei in the excited substate with $M = -1/2$ may decay (according to selection rules) both to the ground substate $m = -1/2$ (figure 2(*b*)) and to $m = +1/2$ (figure 2(*c*)). However, only the radiation resulting from the nuclear transition to the ground substate with $m = -1/2$ contributes to the signal observed (figure 2(*b*)).

Figure 5 shows the results of more detailed studies of the time evolution at the excitation of the nuclear transition $-1/2 \rightarrow -1/2$ (case b in figure 4). The curves were measured at different shifts $\Delta\omega = \omega - \omega_b$ of the incident radiation to the

sides of the resonance. Both positive and negative shifts cause the same increase in transmission at times prior to $t = 0$. On the other hand, the bursts appearing after the magnetization reversal are different. One of them is lower and the other is much higher compared with the incident radiation level. For $\Delta\omega = -3.5\Gamma_0$ ($\Gamma_0 = 0.097$ mm s^{-1} is the natural width of the 14.4 keV excited state in ^{57}Fe) the intensity of the burst is slightly less than that measured in resonance, whereas at $\Delta\omega = +3.5\Gamma_0$ the burst height is well above the incident radiation intensity. It is twice as much as the intensity of γ-radiation absorbed by the target before the magnetic field reversal. The intensity beats have approximately the same period in all three cases considered.

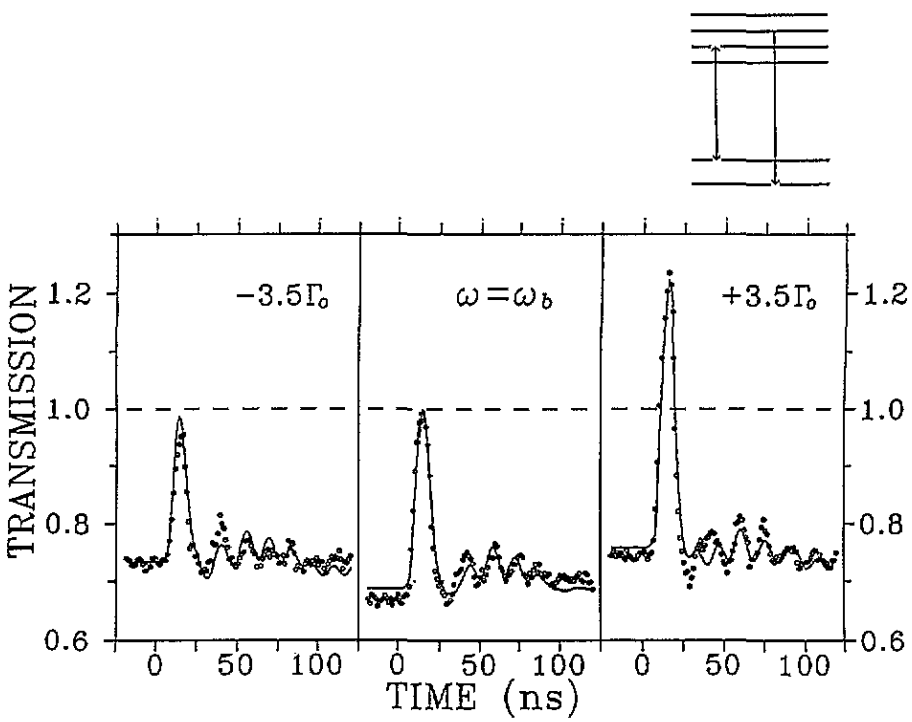

Figure 5. Time evolution of the intensity of γ-rays emerging from the target in the forward direction after excitation of the HF nuclear transition $-1/2 \rightarrow -1/2$ (b) with different detuning $\omega - \omega_b$ from the resonance conditions.

Figure 6 shows the results of similar studies at the excitation of the nuclear transition with opposite magnetic quantum numbers $+1/2 \rightarrow +1/2$ (e). It is interesting to note that the time dependences are similar to those in figure 5 but the whole picture is inverted. Now the most intense first burst appears on the left side of the resonance ($\Delta\omega = -3.5\Gamma_0$) rather than on the right side ($\Delta\omega = +3.5\Gamma_0$). Time dependences in figures 5 and 6 give additional evidence that the magnetization reversal causes a change in the energy of the nuclear excited state and evokes subsequent spontaneous γ-quanta emission at a shifted frequency in the forward direction.

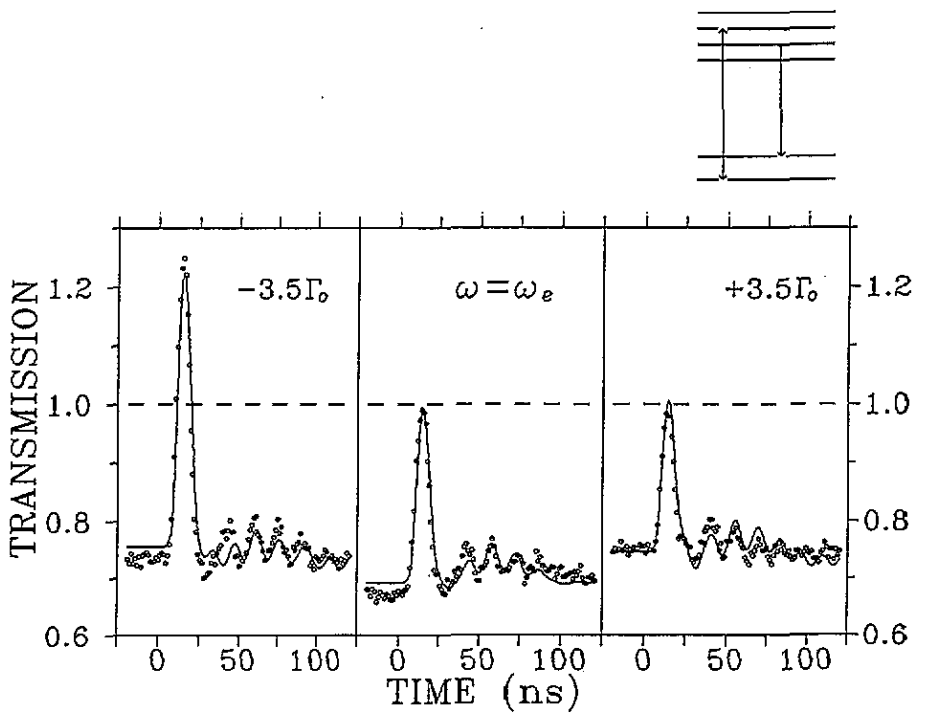

Figure 6. Time evolution of the intensity of γ-rays emerging from the target in the forward direction after excitation of the HF nuclear transition $+1/2 \rightarrow +1/2$ (e) with different detuning $\omega - \omega_b$ from the resonance conditions.

A detailed discussion of the experimental results is carried out in section 4. For this purpose the theory developed in section 3 is used.

3. Theory

To describe the experimental results, we consider a theoretical model in which the HF magnetic field direction is inverted abruptly at time instant $t = 0$. The main purposes of this section are: (i) to calculate the time dependence of resonant γ-radiation propagation in a nuclear system in the forward direction after HF magnetic field reversal and (ii) to formulate the conditions for the feasibility of coherent resonant inelastic γ-quanta scattering by a nuclear system.

The nuclei are located within a slab. The y axis is oriented perpendicular to its surface with the point $y = 0$ at the entrance surface. The incident radiation is a monochromatic plane wave $\mathcal{E}_\omega \exp[i(ky - \omega t)]$ propagating along the y axis with $k = \omega/c$. The radiation wave is modified owing to interaction with the nuclei. Inside the slab the radiation field may be represented as:

$$E(r,t) = E_0(y,t)\exp[i(ky - \omega t)]. \tag{3.1}$$

Here $\boldsymbol{E}_0(y,t)$ is a slowly varying envelope, which does not change practically within the distance of radiation wavelength $\lambda = 2\pi/k$ and during the time $2\pi/\omega$. To calculate the time dependence of coherent γ-radiation propagation in the slowly varying envelope approximation, the wave equation can be used in reduced form (see e.g. [21] for more detail):

$$\frac{\partial \boldsymbol{E}_0(y,t)}{\partial y} = -\frac{2\pi}{c}\boldsymbol{J}_0(y,t) \tag{3.2}$$

$$\boldsymbol{E}_0(0,t) = \mathcal{E}_\omega. \tag{3.3}$$

Here $\boldsymbol{J}_0(y,t)$ is an envelope of the nuclear current density induced by incident radiation:

$$\boldsymbol{J}(\boldsymbol{r},t) = \boldsymbol{J}_0(y,t)\exp[\mathrm{i}(ky-\omega t)]. \tag{3.4}$$

The current density of the whole nuclear system is the sum of the current densities of the individual nuclei. It is convenient to use the momentum representation for its calculations:

$$\boldsymbol{J}(\boldsymbol{r},t) = \int \frac{\mathrm{d}\boldsymbol{k}}{(2\pi)^3}\exp(\mathrm{i}\boldsymbol{k}\cdot\boldsymbol{r})\sum_a \langle\Psi_a(t)|\hat{\boldsymbol{j}}(\boldsymbol{k})|\Psi_a(t)\rangle\exp(-\mathrm{i}\boldsymbol{k}\cdot\boldsymbol{r}_a). \tag{3.5}$$

Here $\boldsymbol{r}_a$ is the radius vector of the ath nucleus; $\langle\Psi_a(t)|$ is a nucleus wavefunction; $\hat{\boldsymbol{j}}(\boldsymbol{k})$ *is the operator of the current density of a nucleus in momentum representation;* and $\langle\Psi_a(t)|\hat{\boldsymbol{j}}(\boldsymbol{k})|\Psi_a(t)\rangle$ is its value.

3.1. Calculation of the current density of an individual nucleus†

We consider a nucleus with a ground state of energy E_g, spin I_g, magnetic moment μ_g and excited state of energy E_e, spin I_e, magnetic moment μ_e (e.g. for ^{57}Fe, $I_g = 1/2$, $I_e = 3/2$, $E_e - E_g = 14.4$ keV)—see figure 2. In the absence of external magnetic and radiation fields the nucleus is described by the unperturbed Hamiltonian $\hat{\mathcal{H}}_0$. For definiteness let us assume, in accordance with experimental conditions, that the HF magnetic field $\boldsymbol{H}_{\mathrm{hf}}(t)$ is directed along the z axis parallel to the surface of the slab. The field changes instantaneously at time $t = 0$ between the values $\boldsymbol{H}_{\mathrm{hf}}$ and $\boldsymbol{H}'_{\mathrm{hf}} = -\boldsymbol{H}_{\mathrm{hf}}$: $\boldsymbol{H}_{\mathrm{hf}}(t) = \boldsymbol{n}_z\boldsymbol{H}_{\mathrm{hf}}\phi(t)$. Here function $\phi(t)$ is introduced, which equals $+1$ for $t \leqslant 0$ and -1 otherwise. The hyperfine interaction $-\boldsymbol{\mu}\cdot\boldsymbol{H}_{\mathrm{hf}}$ splits the nuclear states. Let these substates of a nucleus, which are steady states at negative times, be given by $|m\rangle$ and $|M\rangle$. The Hamiltonian in the presence of an alternating magnetic field is given by

$$\hat{\mathcal{H}}_1(t) = \hat{\mathcal{H}}_0 - \epsilon_\nu\phi(t)\hat{I}_z \tag{3.6}$$

where $\hat{I}_z$ is the operator of a nuclear spin projection onto the z axis and $\epsilon_\nu = \mu_\nu H_{\mathrm{hf}}/I_\nu$ is the hyperfine splitting energy (ν = g,e). The influence of the quadrupole interaction was considered to be not significant in the first approximation. To simplify the theory it was neglected.

† Similar quantum-mechanical techniques were used in [22] for calculating Mössbauer spectra in the presence of a randomly fluctuating magnetic field.

At negative times $\hat{\mathcal{H}}_1$ is time independent and the following relations are valid:

$$\begin{aligned}\hat{\mathcal{H}}_1|m\rangle &= (E_g - \epsilon_g m)|m\rangle \\ \hat{\mathcal{H}}_1|M\rangle &= (E_e - \epsilon_e M)|M\rangle.\end{aligned} \tag{3.7}$$

At positive times after changing the magnetic field direction $\hat{\mathcal{H}}_1$ is time independent as well. The states $|m\rangle$ and $|M\rangle$ are again eigenstates but with eigenenergies changed to $E_g + \epsilon_g m$ and $E_e + \epsilon_e M$ respectively. The formulae (3.6) and (3.7) present the formal description of the possibility of changing the nucleus energy by inverting the magnetic field direction (figure 2).

We are interested in the time behaviour of the interaction of resonant γ-radiation with a nucleus in the presence of a magnetic field that is switched between two opposite directions. To find the solution for nuclear wavefunction $|\Psi_a(t)\rangle$ in this case the full Hamiltonian

$$\hat{\mathcal{H}} = \hat{\mathcal{H}}_1(t) + \hat{V}_a(t) \tag{3.8}$$

with the term $\hat{V}_a(t)$ representing interaction of the ath nucleus with γ-radiation should be considered. In our case it is convenient to present $\hat{V}_a(t)$ in the following form (see e.g. [11], equation (3.8)):

$$\hat{V}_a(t) = \mathrm{i}\omega^{-1}\hat{\jmath}^*(\boldsymbol{k}) \cdot \boldsymbol{E}_0(y_a, t) \exp[\mathrm{i}(\boldsymbol{k} \cdot \boldsymbol{r}_a - \omega t)]. \tag{3.9}$$

The time-dependent perturbation theory was used to calculate $|\Psi_a(t)\rangle$ and $\langle\Psi_a(t)|\hat{\jmath}(\boldsymbol{k})|\Psi_a(t)\rangle$. It is assumed that the intial state of a nucleus at $t = -\infty$ is $|m\rangle$. In the first non-vanishing order of perturbation theory (see e.g. [23]) the current density is given by

$$\begin{aligned}\langle\Psi_a(t)|\hat{\jmath}(\boldsymbol{k})|\Psi_a(t)\rangle = -(\mathrm{i}\hbar)^{-1}&\langle m|\hat{U}_1^+(t,-\infty)|m'\rangle\langle m'|\hat{\jmath}(\boldsymbol{k})|M'\rangle \\ &\times \int_{-\infty}^{t} \mathrm{d}t' \langle M'|\hat{U}_1(t,t')|M\rangle\langle M|\hat{V}_a(t')|m''\rangle\langle m''|\hat{U}_1(t',-\infty)|m\rangle\end{aligned} \tag{3.10}$$

where

$$\hat{U}_1(\tau', \tau'') = \hat{T}\exp\left(-\frac{\mathrm{i}}{\hbar}\int_{\tau''}^{\tau'} \mathrm{d}\tau\, \hat{\mathcal{H}}_1(\tau)\right) \tag{3.11}$$

is the evolution time ordered operator with time ordering given by $\hat{T}$. However, in our case the Hamiltonian at one instant of time τ'' will commute with the Hamiltonian at a later instant τ', $[\hat{\mathcal{H}}_1(\tau'), \hat{\mathcal{H}}_1(\tau'')] = 0$, and hence $\hat{T}$ can be omitted. Everywhere the notation like $|m\rangle\langle m|$ in (3.10) implies the summation over m.

To calculate $\langle\Psi_a(t)|$ and $\langle\Psi_a(t)|\hat{\jmath}(\boldsymbol{k})|\Psi_a(t)\rangle$ it is necessary to find the values of matrix elements of the operator $\hat{U}_1(\tau', \tau'')$. By simple manipulation we get

$$\begin{aligned}\langle m|\hat{U}_1(\tau', \tau'')|m'\rangle &= \delta_{mm'}\exp\{-(\mathrm{i}/\hbar)[E_g(\tau' - \tau'') - \mathrm{i}\epsilon_g m(|\tau'| - |\tau''|)]\} \\ \langle M|\hat{U}_1(\tau', \tau'')|M'\rangle &= \delta_{MM'}\exp\{-(\mathrm{i}/\hbar)[(E_e - \mathrm{i}\Gamma_0\hbar/2)(\tau' - \tau'') - \mathrm{i}\epsilon_e M(|\tau'| - |\tau''|)]\}.\end{aligned} \tag{3.12}$$

These matrix elements show that the magnetic field reversal causes a change of the nuclear sublevel energy, whereas the quantum numbers of spin projections are conserved. In (3.12) we have introduced without explicit calculations the complex energy $E_e - i\Gamma_0\hbar/2$ with the imaginary part describing the nuclear excited-state damping, which originates from the interaction of the nucleus with the field of virtual photons and the electronic shell of an atom.

Substituting (3.9) and (3.12) into (3.10) and averaging over the initial population of nuclear ground substates $|m\rangle$ we obtain the expression for the coherent part of the current density of an individual nucleus:

$$\langle\Psi_a(t)|\hat{j}^s(\kappa)|\Psi_a(t)\rangle = \frac{\Gamma_0}{2\omega(2I_g+1)}\exp[i(\boldsymbol{k}\cdot\boldsymbol{r}_a-\omega t)] \times \sum_{mM}\langle m|\hat{j}^s(\kappa)|M\rangle\langle M|(\hat{j}^{s'})^*(\boldsymbol{k})|m\rangle\exp[if_{mM}(t)t] \times \int_{-\infty}^{t} dt'\exp[-if_{mM}(t')t']E_0^{s'}(y_a,t') \tag{3.13}$$

with parameters

$$f_{mM}(t) = \omega - \omega_{mM}(t) + i\Gamma_0/2 \qquad \omega_{mM}(t) = \omega_0 + \Omega_{mM}\phi(t)$$
$$\omega_0 = (E_e - E_g)\hbar \qquad \Omega_{mM} = (\epsilon_g m - \epsilon_e M)/\hbar. \tag{3.14}$$

The function $\omega_{mM}(t)$ describes the time evolution of a transition frequency between sublevels $\langle M|$ and $\langle m|$ of excited and ground states caused by the magnetic field reversal. Before the reversal the transition frequency equals $\omega_{mM}(-0) = \omega_0 - \Omega_{mM} = \omega_{mM}$, whereas after the reversal it takes on the value $\omega_{mM}(+0) = \omega_0 + \Omega_{mM} = \omega'_{mM}$. Here Ω_{mM} is the relative nuclear transition frequency. Index $s(s') = \pi, \sigma$ in (3.13) and (3.14) labels components of orthogonal polarizations.

3.2. Wave equation

Now we can evaluate the current density of the whole nuclear system. For this purpose we can use equations (3.5), (3.13) and (3.14). Performing summation over all nuclei in the target we get for the coherent part of the current density envelope:

$$J_0^s(y,t) = -\frac{i\omega}{4\pi}\hat{\mathcal{G}}_0^{ss'}(t,t')E_0^{s'}(y,t'). \tag{3.15}$$

Here the causal integral operator $\hat{\mathcal{G}}_0^{ss'}(t,t')$ is introduced, which is defined as

$$\hat{\mathcal{G}}_0^{ss'}E_0^{s'} = -i\frac{\Gamma_0}{2}\sum_{mM} g_0^{ss'}(mM)\exp[if_{mM}(t)t]\int_{-\infty}^{t} dt'\exp[-if_{mM}(t')t']E_0^{s'}(y,t') \tag{3.16}$$

where

$$g_0^{ss'}(mM) = -\frac{8\pi N_0 f_{LM}}{\omega^2(2I_g+1)\Gamma_0}\langle m|\hat{j}^s(\boldsymbol{k})|M\rangle\langle M|(\hat{j}^{s'})^*(\boldsymbol{k})|m\rangle. \tag{3.17}$$

The operator $\hat{\mathcal{G}}_0^{ss'}(t,t')$ carries complete information on the dynamics of the nuclear resonance scattering under the given conditions. The factors N_0 and f_{LM} are defined below.

In the limiting case where the HF field is steady state, (i.e. $\omega_{mM}(t)$ is time independent) and the radiation field $E_0^s(y,t)$ is steady state as well, the causal operator reduces merely to the time-independent value, which has a well known form:

$$\hat{\mathcal{G}}_0^{ss'} = \sum_{mM} \frac{g_0^{ss'}(mM)\Gamma_0/2}{\omega - \omega_{mM} + i\Gamma_0/2}. \tag{3.18}$$

Let us consider for definiteness the M1 type of nuclear transition, which corresponds to the 14.4 keV transition in ^{57}Fe. For this case the matrix elements $\langle m|\hat{j}^s(k)|M\rangle$ were calculated, for example, in [24]. Using those formulae coefficients $g_0^{ss'}(mM)$ are given by:

$$g_0^{ss'}(mM) = \delta^{ss'} g_0^s(mM) \qquad g_0^s(mM) = -g_0 \begin{pmatrix} I_g & 1 & I_e \\ -m & m-M & M \end{pmatrix}^2 3P^s_{m-M}$$

$$g_0 = \frac{\sigma_R N_0}{k} \qquad \sigma_R = \frac{4\pi}{k^2}\frac{\Gamma_{coh}}{\Gamma_0} \qquad \Gamma_{coh} = f_{LM}\frac{2I_e+1}{2(2I_g+1)}\Gamma_1 \tag{3.19}$$

$$P^s_{m-M} = \begin{cases} (n_z \cdot h^s)^2 & m-M=0 \\ \frac{1}{2}[1-(n_z\cdot h^s)^2] & m-M=\pm 1. \end{cases}$$

Here the Mössbauer effect probability was taken into account by introducing the Lamb–Mössbauer factor f_{LM} of recoilless emission and absorption. The quantity N_0 in preceding formulae is the number of nuclei in unit volume;

$$\begin{pmatrix} I_g & 1 & I_e \\ -m & m-M & M \end{pmatrix}$$

is the $3j$-symbol; σ_R is the cross section of γ-resonance absorption; Γ_{coh} is the coherent part of the radiative channel decay width Γ_1; P^s_{m-M} is the polarization factor; and h^s is the linear polarization vector, which is directed along the magnetic vector of the radiation field. The expression for P^s_{m-M} shows that the h^σ polarization component in figure 1 interacts with $m-M=0$ nuclear transitions, while h^π interacts with $m-M=\pm 1$ ones.

Equation (3.2) together with (3.15)–(3.19) comprise the final version of the wave equation for a radiation field traversing the nuclear resonance target in the presence of a magnetic field that is switched between opposite directions at a time instant $t=0$:

$$\frac{\partial E_0^s(y,t)}{\partial y} = i\frac{k}{2}\hat{\mathcal{G}}_0^s(t,t')E_0^s(y,t') \tag{3.20}$$

$$E_0^s(0,t) = \mathcal{E}_\omega^s. \tag{3.21}$$

In steady-state conditions, where the causal operator $\hat{G}_0^s(t,t')$ is given by expression (3.18), the solution of equations (3.20) and (3.21) is straightforward:

$$E_0^s(y,t) = \mathcal{E}_\omega^s R^s(y,\omega)$$

$$R^s(y,\omega) = \exp\left(-i\sum_{mM}\frac{\xi^s_{mM}\Gamma_0}{\omega-\omega_{mM}+i\Gamma_0/2}\right). \tag{3.22}$$

The parameter ξ^s_{mM} is actually the thickness parameter of the absorbing target for the particular hyperfine resonance transition:

$$\xi^s_{mM} = -kg^s_0(mM)y/4. \tag{3.23}$$

It corresponds to the resonance-absorption factor by the relation $m^s_{mM} = 4\xi^s_{mM}$. Expression (3.22) is a typical solution that describes propagation of monochromatic radiation in nuclear resonant media with hyperfine splitting.

It is interesting to note that in those problems where the nuclear states are subjected to time-dependent external perturbations the use of dynamic operators provides the possibility to write down the wave equation in a unified form (equation (3.20)) that is independent of the type of perturbations. For example, in the case of nuclei vibrating in space, the wave equation derived in [11] has the same form as equation (3.20); however, the dynamic operator in that case ([11], equation (3.12)) differs from the dynamic operator obtained in the present paper. The other example is the steady-state conditions, where the dynamic operator reduces merely to the value given by equation (3.18). Thus in each particular case the dynamic operator may take different forms. However, the wave equation has the unified form presented by equation (3.20).

3.3. Solutions of the wave equation

3.3.1. Steady-state HF magnetic field. Prior to solving the general problem expressed by equations (3.20) and (3.21) we shall obtain solutions for a few simpler problems, where a steady-state non-switching HF magnetic field is considered. This means that the transition frequencies $\omega_{mM}(t)$ (equation (3.14)) are time independent. Therefore the explicit time dependence of equation (3.20) disappears. Instead, we introduce time dependence (i) into the boundary condition and (ii) into the right-hand side of the equation by adding a term proportional to some current density $j^s_0(y,t)$:

$$\partial E^s_0/\partial y = \mathrm{i}(k/2)\hat{\mathcal{G}}^s_0 E^s_0 - (2\pi/c)j^s_0 \tag{3.24}$$

$$E^s_0(0,t) = \mathcal{E}^s_\omega \psi(t). \tag{3.25}$$

Hereafter the notation $\hat{\mathcal{G}}^s_0$ is used instead of $\hat{\mathcal{G}}^s_0(t,t')$ to denote the dynamic operator (3.16) with the time-independent frequencies ω_{mM}.

The particular solutions of equations (3.24) and (3.25) will be used later on to derive the general solution in the case in question where the magnetic field is reversed at a certain instant of time.

3.3.2. Non-stationary irradiation of the nuclear target. Let us consider first the case where the current density $j^s_0(y,t)$ is zero, but the incident radiation amplitude is time dependent, so that $\psi(t)$ in (3.25) is an arbitrary complex function of time. The general solution $E^s_0(y,t)$ of this problem was obtained by convolution of the field amplitude $E^s_0(0,t)$ at the entrance surface with a coherent response function $G^s(y,t)$ of the nuclear target [25]:

$$E^s_0(y,t) = \int_{-\infty}^{t} \mathrm{d}t'\, G^s(y,t-t')E^s_0(0,t')\exp[\mathrm{i}\omega(t-t')]. \tag{3.26}$$

The response function $G^s(y,t)$ is defined as the solution of wave equation (3.24) with the boundary condition given by the Dirac delta function: $E_0^s(0,t) = \delta(t)$ and $j_0^s(y,t) = 0$. By using Fourier transformation in time and performing simple manipulations, the following expression for the response function is obtained:

$$G^s(y,t) = \int_{-\infty}^{\infty} \frac{d\omega'}{2\pi} R^s(y,\omega') \exp(-i\omega' t). \tag{3.27}$$

Here $R^s(y,\omega)$ is the spectral function (3.22) of the target in the presence of the steady-state magnetic field on the nuclei. In the particular case where the frequencies ω_{mM} of hyperfine transitions are well separated, the response function can be expressed analytically [25]:

$$G^s(y,t) = \delta(t) - \Gamma_0 \sum_{mM} \xi_{mM}^s \frac{J_1[2(\xi_{mM}^s \Gamma_0 t)^{1/2}]}{(\xi_{mM}^s \Gamma_0 t)^{1/2}} \exp(-i\omega_{mM} t - \Gamma_0 t/2)\theta(t). \tag{3.28}$$

Here J_1 is the Bessel function of the first kind of the first order; $\theta(t)$ is the step function. The excitation of only one resonance transition is considered hereafter unless otherwise stated, i.e. it is assumed that the main frequency of incident radiation ω is close to some specific transition with resonance frequency ω_{mM}: $|\omega - \omega_{mM}| \sim \Gamma_0$. In these conditions only one term can be retained in the sum of equation (3.28).

3.3.3. Time evolution of resonance absorption. Let us calculate as an example the time dependence of γ-radiation transmission through the resonance target provided the incident radiation is switched on at time $t = 0$, i.e. the resonant interaction starts at $t = 0$ as well. This implies that at the entrance surface the radiation amplitude is given by

$$E_0^s(0,t) = \mathcal{E}_\omega^s \theta(t). \tag{3.29}$$

Substituting equations (3.29) and (3.28) into (3.26) we obtain for times $t \ll 1/|\omega - \omega_{mM} + i\Gamma_0/2|$:

$$E^s(y,t) = \mathcal{E}_\omega^s J_0[2(\xi_{mM}^s \Gamma_0 t)^{1/2}] \exp(-i\omega t)\theta(t). \tag{3.30}$$

In the case where $\xi_{mM} \gg 1$ the main processes die out within the considered time interval and thus equation (3.30) is a good approximation to the exact solution. This indicates that, in the first moments after switching on the incident radiation at $t = 0$, the strongly absorbing target does not remove radiation from the incoming beam. Resonant absorption is established with the time delay $\sim \tau_0/\xi_{mM}^s$. This delay depends on thickness parameter ξ_{mM}^s (for the given value of excited nucleus lifetime $\tau_0 = 1/\Gamma_0$) and it can be made much shorter than τ_0. This result was used in [5,18] for the elaboration of the magnetic resonance shutter.

3.3.4. Time evolution of the coherent spontaneous emission. Here we shall consider another example that is of importance for a thorough insight into the transient phenomena occurring for fast HF field reversal.

Consider the case of continuous irradiation of the resonance target. For definiteness let us assume, as previously, that the target possesses a large resonance absorption factor $\xi^s_{mM} \gg 1$. In this case the incident radiation is absorbed nearly completely, according to equations (3.22) and (3.23). Let us assume further that the incident radiation is shut off at $t = 0$. This assumption can be formally expressed by introducing the boundary condition:

$$E^s_0(0,t) = \mathcal{E}^s_\omega \theta(-t). \tag{3.31}$$

On substituting equations (3.31) and (3.28) into (3.26) and performing calculations, we obtain the expression for the amplitude of radiation emerging from the target in the forward direction after the incident beam chopping:

$$E^s(y,t) = -\mathcal{E}^s_\omega J_0[2(\xi^s_{mM}\Gamma_0 t)^{1/2}] \exp(-i\omega_{mM} t)\theta(t). \tag{3.32}$$

Again the formula derived is valid for $t \ll 1/|\omega - \omega_{mM} + i\Gamma_0/2|$ and is a good approximation in the case where $\xi^s_{mM} \gg 1$ (for calculation in the other limiting case $\xi^s_{mM} \simeq 1$, see e.g. [26]). The important thing to note here is that the delayed radiation behind the target is in antiphase with the incident radiation. The latter observation provides evidence that the radiation is a result of re-emission by nuclei.

According to (3.32) a nearly black resonant absorber emits a radiation flash in the forward direction with a peak amplitude that equals the incident radiation amplitude. This reveals the phenomena of *enhancement* of the radiative deday channel in a coherently excited nuclear system [1,2].

The flash duration varies inversely with the thickness parameter τ_0/ξ^s_{mM}, i.e. with the number of nuclei participating in the interaction. In the case where $\xi^s_{mM} \gg 1$, the time behaviour is determined by the Bessel function, rather than by $\exp(-\Gamma_0 t/2)$, and its duration may be much shorter than the natural nucleus lifetime τ_0. The latter effect has a complex nature and originates from (i) the *speed-up decay* of the coherently excited nuclear system [1,2] and (ii) strong resonance absorption of the re-emitted radiation, which develops within time τ_0/ξ^s_{mM} (see e.g. the previous section).

Now we can draw the final conclusion: the nuclear system after switching off the incident radiation emits spontaneously intense radiation in the forward direction within a time domain much shorter than τ_0. Spontaneous emission in the forward direction by coherently excited nuclei was observed recently [5,6].

3.3.5. Internal source of radiation. Let us consider the next particular case. Assume now that the incident radiation is absent, i.e. the boundary condition (3.25) takes on the form $E^s_0(0,t) = 0$. However, an internal source of radiation with plane symmetry exists in the target, i.e. $j^s_0(y,t)$ is no longer zero.

The radiation amplitude at the exit surface of the target may be given by the convolution

$$E^s_0(y,t) = -\frac{2\pi}{c}\int_{-\infty}^{t} dt' \int_0^y dy'\, G^s(y-y', t-t') j^s_0(y',t') \exp[i\omega(t-t')] \tag{3.33}$$

of $j_0^s(y,t)$ with function $G^s(y-y',t-t')$. The function $G^s(y-y',t-t')$ is a fundamental solution of equation (3.24) with zero boundary conditions and with current density given by $-(2\pi/c)j_0^s(y,t) = \delta(y-y')\delta(t-t')$. In other words $G^s(y-y',t-t')$ is the solution of equation (3.24) with the internal plane and prompt radiation source. By using the space–time Fourier transformation of equation (3.24), it can be shown that its fundamental solution coincides with the coherent response function of a nuclear target, which was given by (3.27).

Now let us turn to the solution of equation (3.20). It will be solved easily by using particular solutions obtained in these sections.

3.4. Solution of the wave equation at the HF magnetic field reversal

The solution of equations (3.20) and (3.21) will be represented as a sum of particular solutions at negative $N_0^s(y,t)$ and positive $P_0^s(y,t)$ times, i.e. for times before and after magnetic field reversal:

$$E_0^s(y,t) = N_0^s(y,t) + P_0^s(y,t). \tag{3.34}$$

At negative times the magnetic field on the nuclei is constant and thus the stationary solution given by equations (3.22) and (3.23) is valid:

$$N_0^s(y,t) = \mathcal{E}_\omega^s R^s(y,\omega)\theta(-t).$$

Inserting (3.34) into equations (3.20) and (3.21) with the given expression for $N_0^s(y,t)$, we obtain an equation for $P_0^s(y,t)$, which turns out to coincide with equations (3.24) and (3.25). However, the operator $\hat{\mathcal{G}}_0^s(')$ with the new nuclear transition frequencies ω'_{mM} is used instead of $\hat{\mathcal{G}}_0^s$, since the magnetic field reversal has changed transition frequencies $\omega_{mM} \to \omega'_{mM}$. The performed manipulations result in the appearance of the time-dependent current density $j_0^s(y,t)$:

$$\frac{2\pi}{c} j_0^s(y,t) = \mathcal{E}_\omega^s R^s(y,\omega) \sum_{mM} \frac{i\Gamma_0 \xi_{mM}^s / y}{\omega - \omega_{mM} + i\Gamma_0/2} \exp[i(\omega - \omega'_{mM} + i\Gamma_0/2)t]\theta(t) \tag{3.35}$$

and time-dependent boundary condition $\psi(t)$:

$$\psi(t) = \theta(t). \tag{3.36}$$

Thus equations (3.20) and (3.21) with time-dependent transition frequencies $\omega_{mM}(t)$ are reduced to the inhomogeneous equation (3.24) with the dynamic operator $\hat{\mathcal{G}}_0^s(')$ containing constant frequencies ω'_{mM} as parameters. This transformation and introduction of the time-dependent boundary condition (3.36) implies that beginning with $t = 0$ the incident radiation starts to interact with the new nuclear transition $-m \to -M$, since the relation $\omega \simeq \omega'_{-m-M}$ is valid now (figure 2(*b*)).

The appearance of the time-dependent current density (3.34) in the equation for $P_0^s(y,t)$ actually is evidence for the creation of an internal source of radiation in the target after the reversal of the magnetic field direction at $t = 0$, which is decoupled from the incident radiation. The source is coherent with the incident radiation but radiates at different frequencies. Only one term can be retained in

the sum of equation (3.35), since prior to $t = 0$ the transition $m \to M$ was excited and the relation $\omega \simeq \omega_{mM}$ was valid. In these conditions the new source radiates spontaneously at frequency ω'_{mM}.

The solution of inhomogeneous equation (3.24) with $j_0^s(y,t)$ given by (3.35) and with non-zero boundary condition (3.36) can be represented as the sum of the general solution $F_0^s(y,t)$ of the homogeneous equation with non-zero boundary conditions and the particular solution $S_0^s(y,t)$ of the inhomogeneous equation with zero boundary conditions:

$$P_0^s(y,t) = F_0^s(y,t) + S_0^s(y,t). \tag{3.37}$$

The solution of the homogeneous equation (3.24) with $j_0^s(y,t) = 0$ and non-zero boundary conditions was discussed in section 3.3.2 and is given by equation (3.26). In conjunction with boundary condition (3.36) it describes the time dependence of transmission of radiation through the target provided the interaction with nuclei started at $t = 0$. In the case where the incident radiation is tuned to some specific resonance transition $m \to M$ $(t < 0)$, $F_0^s(y,t)$ is given by

$$F_0^s(y,t) = \mathcal{E}_\omega^s \left\{ 1 - \xi_{mM}^s \Gamma_0 \times \int_0^t \mathrm{d}t' \frac{J_1[2(\xi_{mM}^s \Gamma_0 t')^{1/2}]}{(\xi_{mM}^s \Gamma_0 t')^{1/2}} \exp[\mathrm{i}(\omega - \omega_{mM} + \mathrm{i}\Gamma_0/2)t'] \right\} \theta(t). \tag{3.38}$$

Here we have used that $\xi_{-m-M}^s = \xi_{mM}^s$ and $\omega'_{-m-M} = \omega_{mM}$. Besides if $\xi_{mM}^s \gg 1$ then for $t \ll 1/|\omega - \omega_{mM} + \mathrm{i}\Gamma_0/2|$ the time dependence is given by equation (3.29).

The particular solution $S_0^s(y,t)$ of the inhomogeneous equation with zero boundary conditions was discussed in section 3.3.4 and it is given by formula (3.33). On substituting equations (3.28) and (3.35) into (3.33) and by simple manipulations, we get

$$S_0^s(y,t) = -\mathrm{i}\mathcal{E}_\omega^s \frac{\Gamma_0}{\omega - \omega_{mM} + \mathrm{i}\Gamma_0/2} \exp[\mathrm{i}(\omega - \omega'_{mM} + \mathrm{i}\Gamma_0/2)t]\theta(t) \times \int_0^{\xi_{mM}^s} \mathrm{d}\xi \exp\left(-\mathrm{i}\xi \frac{\Gamma_0}{\omega - \omega_{mM} + \mathrm{i}\Gamma_0/2}\right) J_0\{2[(\xi_{mM}^s - \xi)\Gamma_0 t]^{1/2}\}. \tag{3.39}$$

It is seen that $S_0^s(y,t)$ describes spontaneous emission at shifted frequency. In deriving equation (3.39) the excitation of only one resonance transition $m \to M$ $(t < 0)$ was taken into account. In the limiting case, where $\xi_{mM}^s \gg 1$, that in particular corresponds to the experimental conditions, a little manipulation yields

$$S^s(y,t) = -\mathcal{E}_\omega^s J_0[2(\xi_{mM}^s \Gamma_0 t)^{1/2}] \exp(-\mathrm{i}\omega'_{mM} t)\theta(t). \tag{3.40}$$

Under the condition $\xi_{mM}^s \gg 1$ the latter formula is valid and describes the evolution of spontaneous emission at a shifted frequency. This formula is in substantial agreement with expression (3.32) for the amplitude of radiation for spontaneous coherent emission by nuclei in the forward direction. However, the term $\exp(-\mathrm{i}\omega'_{mM} t)$ appears now instead of $\exp(-\mathrm{i}\omega_{mM} t)$.

The formulae (3.38) and (3.39) describe the time evolution of two main spectral components of radiation that appear behind the nuclear target after HF magnetic field reversal. These formulae are valid provided that the interaction with one resonance transition is taken into account only (one term was retained in equations (3.28) and (3.35)). Otherwise to calculate amplitudes of radiation emerging from the nuclear target the general expressions—equations (3.26) and (3.27) for $F_0^s(y,t)$ and equations (3.33) and (3.35) for $S_0^s(y,t)$—should be used.

3.5. The importance of HF field reversal synchronism

To conclude this section, we would like to comment on the applicability of the expression for current density (3.15), the wave equation (3.20) and the solutions obtained. The formulae (3.15) and (3.20) and the solution obtained for the coherent re-emission with shifted frequency were derived on the assumption of simultaneous HF field reversal on each nucleus at the time instant $t = 0$. It can be shown that in the case of non-synchronized field reversal other expressions for the current density and wave equation should be used, which lead to the violation of coherence in inelastic scattering. Therefore, we can formulate as a sufficient condition for the feasibility of inelastic coherent scattering: *the energy of nuclear states should be changed synchronously at each nucleus*.

However, for inelastic coherent scattering to occur the synchronism of HF field reversal over the entire nuclear system is not necessary. It would be enough if the reversal were synchronous in regions that have size larger than the *coherence volume unit*. The latter is defined (cf. [11]) as the minimal volume containing that number of nuclei which provides a well directed scattering of γ-quanta.

4. Discussion

4.1. Qualitative interpretation of the experimental results

Now we shall analyse the experimental results using the theory developed.

Prior to HF field reversal the incident radiation is in resonance with a certain nuclear transition $m \to M$: $\omega \simeq \omega_{mM}$ and excites the 'white' nuclear subsystem (figure 2(*a*)). After the HF magnetic field reversal the energies of nuclear sublevels in the ground and excited states change (figure 2(*b*)). Under these conditions the incident radiation is in resonance with the new nuclear transition $-m \to -M$: $\omega \simeq \omega'_{-m-M} = \omega_{mM}$. The excitation of the 'black' nuclear subsystem is initiated. Since a finite time is needed for the excitation of the nuclear resonance, the target remains partly transparent for the incident radiation over the time $t \ll \tau_0$. The time dependence of the transmission is described by $F_\omega^s(y,t)$ given by equation (3.38) or by equation (3.30) in the particular case of $\omega \simeq \omega_{mM}$ and a thick target $\xi_{mM}^s \gg 1$; $F_\omega^s(y,t)$ is a decaying function, which has the value $F_\omega^s(y,0) = \mathcal{E}_\omega^s$ at zero time.

The 'white' nuclear subsystem, on the other hand, beginning with $t = 0$ escapes the incident radiation influence and starts to decay spontaneously. The first question is whether it decays coherently or not. To give the real situation more contrast we begin by describing the case in which there is a complete loss of the space–time correlations of amplitudes of nuclear excitations after the HF field reversal. This event may occur either as a result of a localization of the excitation (due to internal conversion, etc.) or as a result of an unsynchronized HF magnetic field reversal at

various nuclei. In this case the secondary γ-radiation would be isotropic and hence it would constitute a negligible fraction of radiation at the detector. Only the radiation at the original frequency ω would contribute substantially to the detector signal. The time behaviour of γ-radiation intensity behind the target would be described by $|F^s_\omega(y,t)|^2$. As a consequence the intensity would reach the same maximum value at the same time, namely at the field reversal time $t = 0$, regardless of the incident radiation frequency. This maximum intensity would coincide with the incident radiation intensity $I^s(0,t) = |\mathcal{E}^s_\omega|^2$. In addition, the time evolution would not have any intensity beats. This model does not agree with the experimental results, so we can discard it. We have to consider a model that takes into account coherent re-emission in the forward direction, i.e. the model considered theoretically in section 3.

According to the theory developed, see e.g. equation (3.37), the radiation that appears behind the target after the HF field reversal is a superposition of two coherent spectral components. The first of them, $F^s(y,t)$, is a result of temporary transparency of the nuclear target and has the original frequency ω. The second one, $S^s(y,t)$, has a shifted frequency ω'_{mM} and results from the coherent spontaneous emission of nuclei. The radiation intensity $I^s(y,t)$ is proportional to

$$|P^s(y,t)|^2 = |F^s(y,t) + P^s(y,t)|^2.$$

We assume first that the incident radiation is tuned exactly to the specific nuclear resonance, i.e. $\omega = \omega_{mM}$. Besides, the target is assumed to be very thick: $\xi^s_{mM} \gg 1$. By using equation (3.30) for $F^s(z,t)$ and equation (3.40) for $S^s(z,t)$ we obtain

$$I^s(y,t) = 4I^s(0,t)J_0^2[2(\xi^s_{mM}\Gamma_0 t)^{1/2}]\sin^2[(\omega_{mM} - \omega'_{mM})t/2]\theta(t). \tag{4.1}$$

It is easily seen that this formula describes the experimental results at least qualitatively.

First, intense radiation appears behind the target. For example, in the case where $|(\omega_{mM} - \omega'_{mM})/2\Gamma_0| \gg \xi^s_{mM} \gg 1$ the peak intensity may exceed the incident radiation intensity level by as much as a factor of 4.

Secondly, the radiation intensity experiences oscillations with period $T_{mM} = 2\pi/|\omega_{mM} - \omega'_{mM}|$. The first intensity peak appears with some delay $t_{mM} \simeq T_{mM}/2$ with respect to time instant $t = 0$. Both the oscillation and time delay depend on the transition $m \to M$ excited and originate from the interference of two spectral components of radiation with equal amplitudes and different frequencies: ω_{mM} and ω'_{mM}.

We must emphasize a very important circumstance here. The nuclear decay may proceed via the radiative channel or the internal conversion channel. For the 14.4 keV transition in the individual ^{57}Fe nucleus the conversion channel dominates and amounts to 89.1%. In the radiative channel the selection rules for an individual nucleus allow transitions to both ground-state sublevels with γ-ray emission at frequencies ω'_{mM} (figure 2(*b*)) and ω'_{-mM} (figure 2(*c*)). However, the theory predicts (see e.g. equation (3.40)) and the present experiment demonstrates that the spontaneous emission proceeds at frequency ω'_{mM} only. The peak amplitude of this component is as large as the incident radiation. This means that the emission at frequency ω'_{mM} is enhanced, whereas the emission at frequency ω'_{-mM} and the internal conversion channel are suppressed.

There is no preference for the ω'_{mM} decay channel over the ω'_{-mM} one in the course of scattering by an individual nucleus. What is the physical meaning of such a

difference between ω'_{mM} and ω'_{-m-M} decay channels in scattering from a system of identical nuclei? The final state in the first channel (figures 2(*a*) and (*b*)) is identical to the initial state (the same spin projection). Note that the energy of this state has changed after the HF field reversal. The initial number of nuclei is conserved in each subsystem. In the other case (figures 2(*a*) and (*c*)), in contrast, one nucleus transfers to the ground state with different spin projection (spin flip), although the energy of this state is identical to the energy of the initial state. One 'white' nucleus becomes 'black', so a tag appears indicating that a certain nucleus re-emitted the γ-quantum at frequency ω'_{-mM}. So, figures 2(*a*) and (*b*) depict the inelastic collective coherent scattering process, while figures 2(*a*) and (*c*) show the individual incoherent one. Thus we can conlude that the observed enhancement of the ω'_{mM} channel is characteristic for coherent nuclear resonance forward scattering. The coherent scattering channel is enhanced, whereas all incoherent ones are suppressed.

From these arguments we can also infer the next condition for the feasibility of coherent inelastic resonant scattering: *the state of a nuclear system prior to and after scattering should remain the same although the energy of this state may change.*

Thirdly, the duration of the radiation flash depends on the nuclear transitions $m \to M$ excited. This takes place because of different effective thicknesses of the target ξ^s_{mM}, which correspond to different nuclear transitions. The larger the thickness parameters ξ^s_{mM} of nuclear transitions involved (in other words the larger the number of nuclei participating in scattering), the shorter the re-emission duration. The thickness dependence of coherent forward scattering was also examined recently in [27] by using synchrotron radiation.

Let us discuss the time dependences presented in figures 5 and 6 where the incident radiation excites nuclear transition above and below resonance. First, according to figure 5, the peak intensity of radiation may change drastically when the nuclei are excited at the resonance side. It is dependent on the value and sign of the detuning parameter $\Delta\omega = \omega - \omega_{mM}$. Secondly, at the excitation of the nuclear transition $-m \to -M$ (figure 6) the whole picture is inverted, i.e. similar time behaviour is obtained when the signs of the detuning parameter and the magnetic quantum numbers are both changed.

Both effects are consistently explained by the theory developed. According to equation (3.39) the re-emitted radiation has the initial phase which depends on detuning parameter $\omega - \omega_{mM}$. Hence, by moving away from the resonance we can influence the conditions of interference of the transmitted and re-emitted radiation. The sooner the constructive interference happens the larger the intensity of the flash. The interference pattern is determined also by the frequency shift $\omega - \omega'_{mM}$ between the two components of the radiation. Therefore if we excite the symmetric nuclear resonance transition $-m \to -M$ the sign of the frequency shift $\omega - \omega'_{-m-M}$ is inverted, which leads to the inversion of the whole picture.

4.2. Quantitative comparison of theory with experiment

The experimental results presented in figures 4–6 were compared with calculations from the theory developed. The incident radiation is assumed to be plane polarized. For all time dependences the intensity was taken to be

$$I^s(L_T, t) = A \int_0^\infty dt' \, D(t') \int_{-\infty}^{\infty} d\omega \, |E^s_\omega(L_T, t - t')|^2 + B. \qquad (4.2)$$

Here A is the intensity factor and B is the background. Function $D(t)$ describes the time resolution of a detector. We use for $D(t)$ the experimental curve measured by the prompt coincidence method with an ^{88}Y radioactive source (see e.g. [28]). The full width at half-maximum of the curve was equal to 5.1 ns. In averaging over ω the spectrum of the incident radiation $|\mathcal{E}^s_\omega|^2$ was assumed to be Lorentzian with width Γ_s.

Function $E^s_\omega(L_T, t-t')$ is given by equations (3.34) and (3.37). The solutions (3.38) for $F^s_\omega(L_T, t-t')$ and (3.39) for $S^s_\omega(L_T, t-t')$ were used in preliminary calculations. These formulae were derived under the assumption that both incident and re-emitted radiation components interact with one resonance transition only. The calculation showed the main effects (e.g. in figure 4) to be described in this approximation already. However, the interaction with the other hyperfine transitions, although weak, turned out to be important. The effect of resonance interaction with neighbouring hyperfine transitions, although small for an isolated nucleus, can be accumulated while the radiation propagates through a thick nuclear target. This causes a noticeable phase shift†. The additional phase shifts turned out to be different for shifted and unshifted spectral components. Thus they cause substantial change of the interference patterns of the two spectral components. For this reason the intensity of the first peak may change markedly, especially in the cases of figures 5 and 6.

The experimental results are compared with theoretical dependences calculated with allowance for the interaction of γ-radiation with neighbouring resonances as well. Numerical calculations using the general expression of equations (3.26) and (3.27) for $F^s_\omega(L_T, t-t')$ and equations (3.33) and (3.35) for $S^s_\omega(L_T, t-t')$ were performed. The results of calculations are shown in figures 4–6.

The experimental time dependences are fitted best by using the following parameters. The intensity and background parameters are: $A = 0.33 \pm 0.02$ and $B = 0.67 \pm 0.03$. The HF parameters Ω_{mM} (equation (3.14)) are: $\Omega_a = -53.3\Gamma_0$, $\Omega_b = -31.1\Gamma_0$, $\Omega_c = -8.4\Gamma_0$ ($\Gamma_0 = 7.087$ MHz). The corresponding values derived from the Mössbauer spectrum in figure 2(*b*) are: $-52.7\Gamma_0$, $-30\Gamma_0$ and $-8\Gamma_0$. The thickness parameters ξ_{mM} are: $\xi_a = 7.7$, $\xi_b = 10.3$, $\xi_c = 2.6$. Only ξ_b was a varying parameter, in fact. The others were calculated using the relation $\xi_a : \xi_b : \xi_c = 3:4:1$, which stems from the same relation for the strength of corresponding resonance transitions at the given magnetization and scattering geometry. The thickness parameters derived from the fitting procedure are in good agreement with the value calculated from equation (3.23): $\xi_b = 10.9$. In the latter case $y = L_T = 17$ μm was used as the target thickness, which was determined from x-ray absorption measurements. The value $g^s_0(mM)$ is calculated by using equation (3.19) and the $FeBO_3$ data (see e.g. [30]). In view of $f_{LM} = 0.95$ and 95% abundance of ^{57}Fe nuclei in the crystal the value $g^\pi_0(b) = 3.52 \times 10^{-5}$.

The effective spectral width of incident radiation was found to be $\Gamma_s = 3.95\Gamma_0$. It is twice as large as the value measured directly (see section 2). By using the increased value of Γ_s we took effectively into account the low-frequency (~ 1 MHz) magnetoacoustic vibrations excited in the nuclear target by the pulsed magnetic fields. The possible high-frequency magnetoacoustic vibrations (~ 100 MHz) were not taken into account in our calculations. This could be the reason for some discrepancies between experimental spectra and theoretical curves in the figures.

† For the first time the weak interaction with neighbouring hyperfine transitions was noticed to be important in the Laue diffraction quantum beat time spectra [29].

In general we may conclude that the theoretical model developed in this paper adequately describes our experimental results.

5. Conclusions

The coherent nuclear scattering of γ-rays in the forward direction by a system of identical nuclei was studied under the conditions of abrupt change of the nuclear excitation energy. The energy of the excited state was changed by fast reversal of the HF magnetic field. The experimental data show that after the field reversal the excited nuclear system decays spontaneously with highly directional emission of γ-quanta in the forward direction at a shifted frequency. The probability of re-emission into the radiative channel increases drastically. The features observed point to the coherent origin of the inelastic re-emission of γ-quanta after the HF field reversal.

The theory describing γ-radiation propagation in resonant nuclear media at an HF field reversal was developed. A number of particular solutions pertinent to the experiment considered were obtained. The theory fits the experiment adequately.

The investigations carried out have shown that the coherent ineleastic γ-resonance scattering is feasible if: (i) the energy of nuclear states is changed synchronously at each nucleus; (ii) the state of the nuclear system prior to and after the scattering remains the same, although the energy of these states may change.

References

[1] Trammell G T 1961 *Chemical Effects of Nuclear Tranformations* vol 1 (Vienna: IAEA) p 75

[2] Afanas'ev A M and Kagan Yu 1965 *Pis. Zh. Eksp. Teor. Fiz.* **2** 130 (Engl. Transl. 1965 *JETP Lett.* **2** 81)

[3] Smirnov G V 1986 *Hyperfine Interact.* **27** 203
van Bürck U 1986 *Hyperfine Interact.* **27** 219

[4] Rüffer R, Gerdau E, Gröte M, Hollatz R, Röhlsberger R, Rüter H D and Sturhahn W 1992 *Hyperfine Interact.* **61** 1279

[5] Shvyd'ko Yu V, Smirnov G V, Popov S L and Hertrich T 1991 *Pis. Zh. Eksp. Teor. Fiz.* **53** 69 (Engl. Transl. 1991 *JETP Lett.* **53** 69)

[6] Hastings J B, Siddons D P, van Bürck U, Hollatz R and Bergmann U 1991 *Phys. Rev. Lett.* **66** 770

[7] Afanas'ev A M and Kagan Yu 1965 *Zh. Eksp. Teor. Fiz.* **48** 327 (Engl. Transl. 1965 *Sov. Phys.–JETP* **21** 215)

[8] Artem'ev A N, Sklarevskii V V, Smirnov G V and Stepanov E P 1972 *Zh. Eksp. Teor. Fiz.* **63** 1390 (Engl. Transl. 1972 *Sov. Phys.–JETP* **36** 736)

[9] Artem'ev A N, Smirnov G V and Stepanov E P 1968 *Zh. Eksp. Teor. Fiz.* **54** 1028 (Engl. Transl. 1968 *Sov. Phys.–JETP* **27** 547)

[10] Popov S L, Smirnov G V and Shvyd'ko Yu V 1989 *Pis. Zh. Eksp. Teor. Fiz.* **49** 651 (Engl. Transl. 1989 *JETP Lett.* **49** 747)
Popov S L, Smirnov G V and Shvyd'ko Yu V 1990 *Hyperfine Interact.* **58** 2463

[11] Shvyd'ko Yu V and Smirnov G V 1992 *J. Phys.: Condens. Matter* **4** 2663

[12] Shvyd'ko Yu V, Popov S L and Smirnov G V 1991 *Pis. Zh. Eksp. Teor. Fiz.* **53** 217 (Engl. Transl. 1991 *JETP Lett.* **53** 231)

[13] Kotrbova M, Kadeckova S, Novak J, Bradler J, Smirnov G V and Shvyd'ko Yu V 1985 *J. Cryst. Growth* **71** 607

[14] Kurtzig A J, Wolfe R, LeCraw R C and Nielsen J W 1969 *Appl. Phys. Lett.* **14** 350

[15] Eibchütz M, Pfeiffer L and Nielsen J W 1970 *J. Appl. Phys.* **41** 1276

[16] Petrov M P, Paugurt A I, Smolenskii G A and Chizhov M K 1972 *Izv. Akad. Nauk Ser. Fiz.* **36** 1472 (Engl. Transl. 1972 *Bull. Acad. Sci. USSR* **36** 1305)

[17] Kolotov O S, Pogozhev V A, Smirnov G V, Shvyd'ko Yu V, Kadečkova S, Kotrbova M and Novak J 1982 *Phys. Status Solidi* a **72** K197–201
[18] Smirnov G V, Shvyd'ko Yu V, Kolotov O S, Pogozhev V A, Kadečkova S, Kotrbova M and Novak J 1984 *Zh. Eksp. Teor. Fiz.* **86** 1495 (Engl. Transl. 1984 *Sov. Phys.–JETP* **59** 875)
[19] Shvyd'ko Yu V, Hertrich T, Sedov V E, Smirnov G V, van Bürck U, Mössbauer R L and Chumakov A I 1992 *Europhys. Lett.* **19** 723
[20] Smirnov G V and Shvyd'ko Yu V 1986 *Pis. Zh. Eksp. Teor. Fiz.* **44** 431 (Engl. Transl. 1986 *JETP Lett.* **44** 556)
[21] Allen L and Eberly J H 1975 *Optical Resonance and Two-Level Atoms* (New York: Wiley) part I, section 6
[22] Blume M and Tjon J A 1968 *Phys. Rev.* **165** 446
[23] Messiah A 1993 *Quantum Mechanics* vol 2 (Amsterdam: North-Holland) ch XVII
[24] Kagan Yu and Afanas'ev A M 1973 *Z. Naturf.* **28a** 1351
[25] Kagan Yu, Afanas'ev A M and Kohn V G 1979 *J. Phys. C: Solid State Phys.* **12** 615
[26] Shvyd'ko Yu V and Smirnov G V 1990 *Nucl. Instrum. Methods* B **51** 452
[27] van Bürck U, Siddons D P, Hastings J B, Bergmann U and Hollatz R 1992 *Phys. Rev.* B **46** 6207
[28] Lynch F J 1966 *IEEE Trans. Nucl. Sci.* **NS-13** 140
[29] Chumakov A I, Smirnov G V, Zelepukhin M V, van Bürck U, Gerdau E, Rüffer R and Rüter H D 1992 *Europhys. Lett.* **17** 269
[30] van Bürck U, Smirnov G V, Mössbauer R L, Maurus H J and Semioschkina N A 1980 *J. Phys. C: Solid State Phys.* **13** 4511